IET Intelligent Transport Systems

Research Article

IET Journals
The Institution of Engineering and Technology

Two-step method to reduce metro transit energy consumption by optimising speed profile and timetable

ISSN 1751-956X
Received on 25th February 2019
Revised 13th February 2020
Accepted on 16th March 2020
E-First on 13th July 2020
doi: 10.1049/iet-its.2019.0103
www.ietdl.org

Bo Jin[1], Pengfei Sun[1] ✉, Qingyuan Wang[1], Xiaoyun Feng[1]

[1]*School of Electrical Engineering, Southwest Jiaotong University, Chengdu 610031, People's Republic of China*

✉ *E-mail: spf0325@163.com*

Abstract: With the rising energy prices and increasing environmental awareness, the energy efficiency of metro transit system has attracted much attention in recent years. This study proposes a two-step optimisation method to optimise speed profile and timetable, aiming to reduce the operational energy consumption of metro transit system. First, a coasting point searching algorithm is designed to reduce tractive energy consumption by optimising speed profile and running time distribution scheme. Then, a mixed-integer linear programming model is constructed to maximise the overlap time between the accelerating and braking phases by optimising headway and dwell time, in order to improve the utilisation of regenerative braking energy (RBE). Furthermore, numerical simulations are presented based on the data from a Guangzhou Metro Line. The results show that the tractive energy consumption can be reduced by 8.46% and the utilisation of RBE can be improved by 11.6%.

Nomenclature

x	train running position, m
t	train running time, s
v	train running speed, m/s
M	mass of train, t
ρ	factor considering the rotating mass
F	train traction force, kN
B_E	train regenerative braking force, kN
B_A	train air braking force, kN
W_0	basic resistance, kN
W_j	line resistance, kN
J_r	total tractive energy consumption, kJ
J_{RBE_a}	total available regenerative braking energy, kJ
J_{RBE_u}	utilised regenerative braking energy, kJ
μ	utilisation rate of regenerative braking energy
i, j	symbol of station
n, m	symbol of train
K	number of stations
S_i	position of station i, m
η	efficiency of the train motor
V_{lim}	speed limit, m/s
T_i	running time of inter-station $[S_i, S_{i+1}]$, s
T_t	total running time, s
T_{sup}	total running time supplement, s
$D_{n,i}$	departure time of train n at station i, s
$A_{n,i}$	arrival time of train n at station i, s
$t_{a,i}$	accelerating time of inter-station $[S_i, S_{i+1}]$, s
$t_{b,i-1}$	braking time of inter-station $[S_{i-1}, S_i]$, s
t_{ov}	overlap time, s
T_{ov}	total overlap time, s
$T_{\text{d},i}$	dwell time at station i, s
T_{safe}	minimum safe headway, s
δ, η	logical variables
α, β	auxiliary variables

1 Introduction

Metro transit system is developing rapidly because of its enormous transportation capability and high convenience. However, with the rising energy prices and increasing environmental awareness, the huge energy consumption of metro transit system has become a non-negligible challenge. Especially, the operational energy consumption of trains accounts for 50% of the total energy consumption of the system [1]. Therefore, many researchers pay attention to reducing the operational energy consumption, among which energy-efficient train control (EETC) and energy-efficient train timetabling (EETT) are mainly concerned [1, 2].

EETC aims at calculating the energy-efficient speed profile of a train journey between two successive stations under pre-given running time (PRT). The energy-efficient speed profile is calculated based on train data (e.g. train mass and tractive characteristics) and line data (e.g. gradient and speed limit), which are used for finding a driving strategy to reduce the tractive energy consumption. In 1968, Ishikawa [3] firstly proposed a simplified train control optimisation problem on a level track and put forward that the optimal train driving strategy consisted of four phases: maximum acceleration (MA), cruising (CR), coasting (CO) and maximum braking (MB). The optimisation model was solved based on Pontryagin's maximum principle (PMP). The Scheduling and Control Group of South Australia (SCG) conducted the EETC research based on PMP [4–6]. Speed limit [4], gradient [5] and steep gradient [6] were introduced into the EETC problem. On the other hand, there are many different methods to solve the EETC problem. Franke *et al.* [7] developed an energy-efficient speed profile optimisation model to minimise the tractive energy consumption. Meanwhile, a discrete dynamic programming algorithm was proposed to solve the non-linear train control problem. Wang *et al.* [8] transformed the non-linear EETC problem into a mixed-integer linear programming (MILP) model, in which the non-linear train model was approximated by a piece-wise affine model. Zhao *et al.* [9] proposed an enhanced Brute force searching method to get the optimal train speed profile, and a field test of the optimal speed profile was presented. The field test results showed that, by implementing the optimal speed profile, the tractive energy consumption can be significantly reduced. Meta-heuristic is also applied to solve the optimisation problem, such as genetic algorithm [10] and ant colony optimisation [11]. According to the short distance between stations and simple line condition of the metro transit system, the coasting point searching algorithm is applied to find the energy-efficient driving strategy. Since the train in the coasting (CO) phase does not consume tractive energy, adding CO phases into the speed profile is an effective way to reduce the tractive energy consumption. The key to the coasting point searching algorithm is to find the starting points of coasting (CO) phases. Wong and Ho [12] optimised the train driving

strategy by using appropriate coasting control. The initiating position of the CO phase was calculated by several searching methods. Similarly, Chang and Sim [13] proposed an optimisation method to solve the EETC problem based on the coasting point searching algorithm, where the genetic algorithm was applied to find the coasting point. The results showed that the tractive energy consumption can be reduced by adding CO phases.

Considering the EETC problem of a train journey with multiple inter-stations (i.e. operating range between two successive stations), Su *et al.* [14] analysed the relationships between running times and tractive energy consumption of each inter-station. An energy-efficient running time distribution scheme was calculated based on the relationship to reduce the total tractive energy consumption of the train journey. The optimisation of running time distribution scheme is part work of the EETT problem, which aims to reduce total tractive energy consumption by adjusting running times. Sicre *et al.* [15] obtained the relationships between running times and tractive energy consumption of each inter-station from a single train simulator. Then, the authors formulated an energy-efficient timetable optimisation model to distribute running times according to the relationship. Vandanjon *et al.* [16] proposed a method capable of producing a set of running times with associated tractive energy consumption that can be used to guide the running time distribution. However, these studies [3–16] ignore the utilisation of regenerative braking energy (RBE), which takes 33% of the total tractive energy consumption [17].

The regenerative braking system is widely used in metro transit system, which can convert the kinetic energy into RBE [1]. The RBE can be fed back to the overhead contact line, where it can be consumed by other accelerating trains in the same substation (i.e. power supply zone). However, if there is no accelerating train, the RBE will be wasted by resistance. To improve the utilisation of RBE, most of the studies focus on synchronising the accelerating and braking phases of trains. Liu *et al.* [18] developed a cooperative train control model to synchronise the accelerating and braking phases of two successive trains. The headway of the latter train was adjusted to improve the utilisation of RBE. Albrecht [19] proposed an approach to adjust the running time for cooperating the operation of trains. The results showed that the utilisation of RBE can be improved by adjusting running times, which can significantly reduce the operational energy consumption of multiple trains. To simplify the cooperative control model, the overlap time between the accelerating and braking phases is investigated for measuring the utilisation of RBE [20]. Then, the synchronisation of accelerating and braking phases is realised by maximising the overlap time in [21, 22]. Yang *et al.* [21] researched the energy-efficient timetable problem to coordinate the operation of trains. The strategy was to adjust headway and dwell time to enhance the overlap time between the accelerating and braking phases.

Combining EETC with EETT, many studies on reducing energy consumption have been developed. Li and Lo [23] built an integrated energy-efficient operation model. In their model, the timetable and the speed profile were optimised jointly taking into account the headway. The timetabling part of the model tried to synchronise the accelerating and braking phases of trains in order to utilise RBE. Meanwhile, the speed profile part optimised the driving strategy to minimise net energy consumption. Zhao *et al.* [24] applied an integrated model for the whole operational day, in which substation energy supply was reduced significantly by adjusting running time and headway. The results showed that the combination of EETC and EETT can reduce more substation energy consumption compared with EETC. In view of the fact that passenger service quality is strongly affected by timetable, bi-objective models are formulated to trade-off energy consumption and passenger service quality in [25, 26]. Yang *et al.* [25] presented a bi-objective model to determine the energy-efficient timetable and speed profile for reducing energy consumption and passenger waiting time. Gao *et al.* [26] designed a bi-objective model to trade-off energy consumption and passenger travel time of express/local stop mode. Owing to the change of onboard passengers, the variations of train mass was considered in the integrated model [27]. More related to our work, a two-step optimisation method considering both the optimisation of speed profile and the efficient utilisation of RBE was built in [28]. Firstly, the authors designed a numerical algorithm to calculate optimal speed profiles according to the PRTs. Then, a cooperative train control model was built to adjust the departure times of accelerating trains for improving the utilisation of RBE. Similarly, Ning *et al.* [22] proposed a two-step approach comprising the distribution of running time and the effective utilisation of RBE. A running time distribution model was first constructed to distribute the running times of each inter-stations in order to minimise the total tractive energy consumption. Then, an RBE utilisation model was obtained by maximising the overlap time between the accelerating and braking phases of multiple trains. A comparison between this paper and the existing literature is given in Table 1. Compared with related studies, the main contributions of this paper are as follows:

Table 1 Literature combining EETC and EETT

Literature	Adjusted timetable parameters	Objectives	Method
Li and Lo [23]	headway	operational energy consumption	GA
Zhao *et al.* [24]	headway, running time	operational energy consumption	brute force algorithm, GA
Yang *et al.* [25]	running time	operational energy consumption passenger waiting time	Taylor approximation
Gao *et al.* [26]	headway, dwell time, running time	operational energy consumption passenger travel time	linear programming
Zhou *et al.* [27]	headway, running time	operational energy consumption	brute force algorithm, NS-GSA algorithm
Su *et al.* [28]	dwell time	tractive energy consumption RBE utilisation	numerical algorithm, bisection method
Ning *et al.* [22]	headway, dwell time, running time	tractive energy consumption overlap time	GA, heuristically iterative algorithm
this paper	headway, dwell time, running time	tractive energy consumption overlap time	coasting point searching algorithm, MILP

GA: genetic algorithm; NS-GSA: genetic annealing algorithm with neighbourhood search strategy; MILP: mixed-integer linear programming.

(i) A novel coasting point searching algorithm is proposed to optimise the speed profiles and running time distribution scheme of a train journey with multiple inter-stations. CO phases are added according to the relationship between running time and tractive energy consumption to reduce the total tractive energy consumption of multiple inter-stations.
(ii) The calculation of overlap time between two successive trains is discussed in detail, which is divided into 12 different cases. The non-linear computational equation of the total overlap time between multiple trains is transformed into a linear expression by introducing logical and auxiliary variables, then the model for maximising overlap time is rebuilt into a MILP model. The MILP model can be solved more efficiently compared with heuristic algorithms because the branch-and-bound algorithms implemented in several existing commercial and free solvers to solve MILP model (CPLEX Solver in this paper).

The remaining of this paper is structured as follows. In Section 2, the framework of the two-step optimisation model is illustrated. In Section 3, the model and algorithm are introduced for minimising

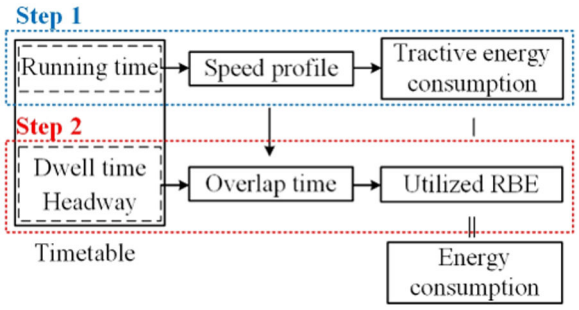

Fig. 1 *Relationship between timetable and energy consumption*

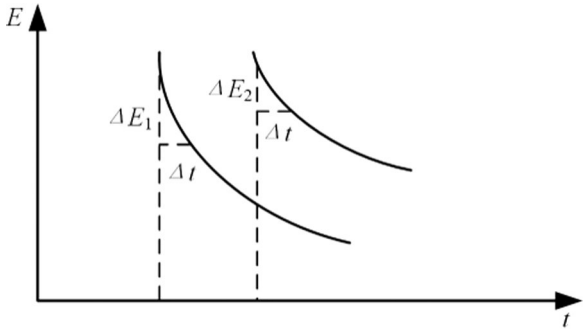

Fig. 2 *Curves of tractive energy consumption versus running time*

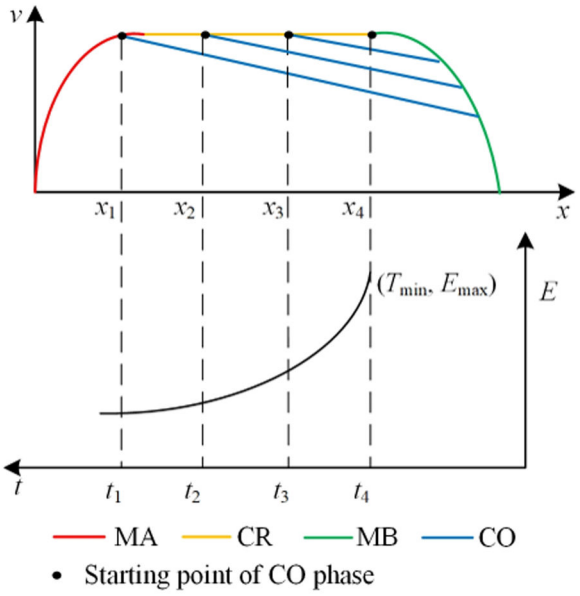

Fig. 3 *Energy-efficient speed profiles and related tractive energy consumption under different running times*

the tractive energy consumption. In Section 4, the MILP model is proposed to maximise the overlap time between the accelerating and braking phases. In Section 5, simulations based on a Guangzhou Metro Line are demonstrated to verify the feasibility of the two-step optimisation method. Conclusions are given in Section 6.

2 Problem statement

The train operational energy consumption is equal to the tractive energy consumption minus the utilised RBE, as shown in Fig. 1. Thus, the total operational energy consumption can be effectively reduced by minimising the tractive energy consumption and maximising the utilisation of RBE.

The optimisation of train speed profile is an effective way to minimise the tractive energy consumption by using energy-efficient driving strategy. Running time has a significant impact on the energy-efficient driving strategy [14]. Running time consists of two parts: minimum running time and running time supplement. Running time supplement is the extra running time on top of minimum running time, which is included in the timetable to manage disturbances [29]. It is worth mentioning that adding the same running time supplement into different inter-stations will cause different reduction of tractive energy consumption [14], as shown in Fig. 2. Therefore, an energy-efficient running time distribution scheme can be obtained by adding running time to the inter-station with a maximum reduction of tractive energy consumption, which determines the running times of each inter-station. Meanwhile, the energy-efficient speed profiles of each inter-station are determined based on the running times.

In another aspect, the utilisation of RBE can be improved by making more trains accelerating and braking at the same time [20]. This idea can be realised by maximising the overlap time between the accelerating and braking phases of trains in the same substation. In addition, adjusting dwell times and headway is an efficient approach to overlap accelerating and braking phases [22].

A two-step optimisation model is proposed to obtain energy-efficient speed profile and timetable, as shown in Fig. 1. In step 1, the speed profile and running time distribution scheme are optimised to minimise the tractive energy consumption. In step 2, the overlap time between the accelerating and braking phases is maximised by adjusting headway and dwell times to improve the utilisation of RBE.

The main notions used throughout the remainder of this paper are introduced in Nomenclature section. This paper makes use of the following assumptions:

(1) In metro transit system, there is no disturbance and all trains keep their service under the timetable in operation.
(2) The adjustment of running times, dwell times and headway has no impact on the passenger transport service.
(3) It is assumed that the power supply system is ideal, and the auxiliary power consumption is assumed to be fixed.
(4) The total running time is constant, which is equal to the travel time from the starting station to the terminal station minus the total dwell time.
(5) Overlap time of successive trains in the same direction is considered. However, the overlap time of trains in the opposite direction is not discussed in this paper.
(6) The efficiency of the train motor is considered as a constant in this paper.

3 Minimising tractive energy consumption

In this section, the optimisation of energy-efficient speed profile is discussed, and the relationship between running time and tractive energy consumption is analysed. A novel coasting point searching algorithm is proposed to get energy-efficient running time distribution scheme and related speed profiles of a train journey with multiple inter-stations.

3.1 Energy-efficient speed profile

The classic energy-efficient train control strategy always consists of four phases: MA, CR, CO and MB [3]. Running time is a vital parameter which influences the combination of these phases [14]. As shown in Fig. 3, when the running time increases, the starting point of the CO phase moves backwards, and the tractive energy consumption decreases. Under the condition of the minimum running time ($T_{\min}$), there is no CO phase in energy-efficient speed profile. This kind of speed profile is called MaxPow speed profile with the maximum tractive energy consumption ($E_{\max}$). When the running time is pre-given, there is a speed profile with the minimum tractive energy consumption, which can be obtained by adding CO phases into the MaxPow speed profile [12]. Therefore, the calculation of the energy-efficient speed profile is about finding the starting points of CO phases. However, the MaxPow speed profile will be complex in the condition of low-speed limit and varying gradient, which makes it difficult to add CO phases to the MaxPow speed profile. This situation is considered in the proposed speed profile optimisation method.

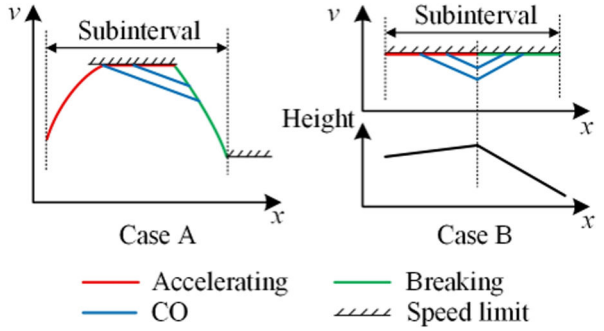

Fig. 4 *Sketch of the formulation of subinterval*

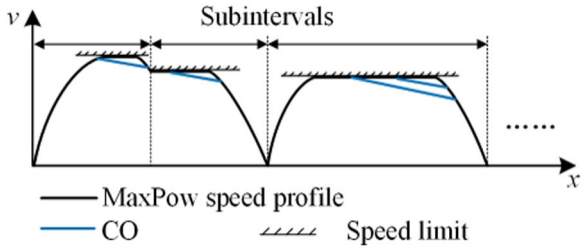

Fig. 5 *Sketch of coasting point searching algorithm*

For a train journey with multiple inter-stations, the running times of each inter-station should be larger than the minimum running time. Therefore, total running time supplement T_{sup} is equal to total PRT minus the sum of minimum running times of each inter-station, described as

$$T_{\text{sup}} = T_t - \sum_{i=1}^{K} T_{i,\min} \tag{1}$$

Running time supplement can be added to any inter-station, but the tractive energy consumption reduction of each inter-station is different, as shown in Fig. 2. The proposed speed profile optimisation method can properly distribute the total running time supplement according to the relationship between running time and tractive energy consumption, thus reducing the total tractive energy consumption of the train journey. Meanwhile, the energy-efficient speed profiles of each inter-station can be obtained.

3.2 Model of minimising tractive energy consumption

The dynamics model of train motion can be formulated as the following continuous-position equation:

$$\begin{cases} M\rho \cdot v\dfrac{\mathrm{d}v}{\mathrm{d}x} = F(v) - B_E(v) - B_A(v) - W_0(v) - W_j(x) \\ \dfrac{\mathrm{d}t}{\mathrm{d}x} = \dfrac{1}{v} \end{cases} \tag{2}$$

additionally

$$W_0(v) = a + bv + cv^2 \tag{3}$$

$$W_j(x) = Mg \cdot \theta(x) + F_c(r(x)) \tag{4}$$

$$F_c(r(x)) = k/r(x) \cdot M \tag{5}$$

where the coefficients a, b and c depend on the train characteristics, which can be calculated from experimental data, $\theta(x)$ is the slope (‰), F_c is the curve resistance (kN), $r(x)$ is the radius of the curve (m) and the coefficient k depends on the track gauge.

In regard to a metro line consisting of $K+1$ stations, the objective function of minimising total tractive energy consumption can be described as

$$\min J_t = \sum_{i=1}^{K} \int_{S_i}^{S_{i+1}} \left(\frac{F(v)}{\eta}\right) \mathrm{d}x \tag{6}$$

subject to the following constraints:

$$\begin{cases} 0 \le F(v) \le F_{\max}(v) \\ 0 \le B_E(v) \le B_{E,\max}(v) \\ 0 \le B_A(v) \le B_{A,\max}(v) \\ 0 \le v \le V_{\lim} \\ v(S_i) = 0 \\ T_{i,\min} \le t(S_{i+1}) - t(S_i) \le T_{i,\max} \\ t(S_{K+1}) - t(S_1) \le T_t \end{cases} \tag{7}$$

where $F_{\max}$ is the maximum traction force (kN), $B_{E,\max}$ is the maximum regenerative braking force (kN), $B_{A,\max}$ is the maximum air braking force (kN), $T_{i,\min}$ and $T_{i,\max}$ are the minimum running time and maximum running time of inter-station $[S_i, S_{i+1}]$, respectively, (s).

3.3 Coasting point searching algorithm

In the condition of low-speed limit and varying gradient, the MaxPow speed profile consists of multiple running processes starting with accelerating phase and ending with braking phase. This kind of running process is defined as subinterval, where CO phase can be added to. According to low-speed limit and varying gradient, the formation of subinterval can be divided into two cases, as shown in Fig. 4. In Case A, the braking phase is taken to meet the constraint of a low-speed limit. Especially, stopping at the station can be considered as a low-speed limit, which is equal to zero. In Case B, the braking phase is taken to keep speed when there is a steep downhill.

To reduce the tractive energy consumption of a train journey with multi inter-stations, a coasting point searching algorithm is proposed as follows.

Coasting point searching algorithm:

1. Calculate the MaxPow speed profiles of each inter-station using a driving strategy combining of MA, CR and MB, in order to get close to the speed limit.
2. Calculate the minimum running time of each inter-station $T_{i,\min}$ and the total running time supplement T_{sup}.
3. Divide the speed profile of the journey into several subintervals.
4. Add CO phases to each subinterval by temporarily moving the starting points of CO phases with step Δx backward.
5. Calculate the running time variation Δt and the tractive energy consumption variation ΔE of each subinterval.
6. Choose the subinterval with maximum $\Delta E/\Delta t$ and add CO phase into this subinterval.
7. Update T_{sup} as $T_{\text{sup}} = T_{\text{sup}} - \Delta t$, if $T_{\text{sup}} > 0$, return to step 3, else end.
8. where the calculation of speed profile is based on (2).

In the proposed coasting point searching algorithm, the speed profile of the journey is divided into several subintervals, as shown in Fig. 5. The strategy is to add CO phase to the subinterval with better energy-saving effect. Meanwhile, running time supplement is distributed to the subinterval with more energy consumption reduction. Finally, an energy-efficient running time distribution scheme and related speed profiles can be obtained.

4 Maximising the utilisation of RBE

The overlap time between the accelerating and braking phases of trains in the same substation is taken as an important indicator to measure the utilisation of RBE. In this section, the overlap time is maximised to improve the utilisation of RBE. The model of

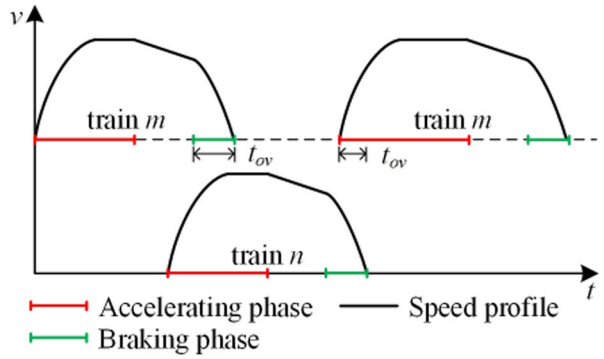

Fig. 6 *Sketch of the overlap time between two successive trains*

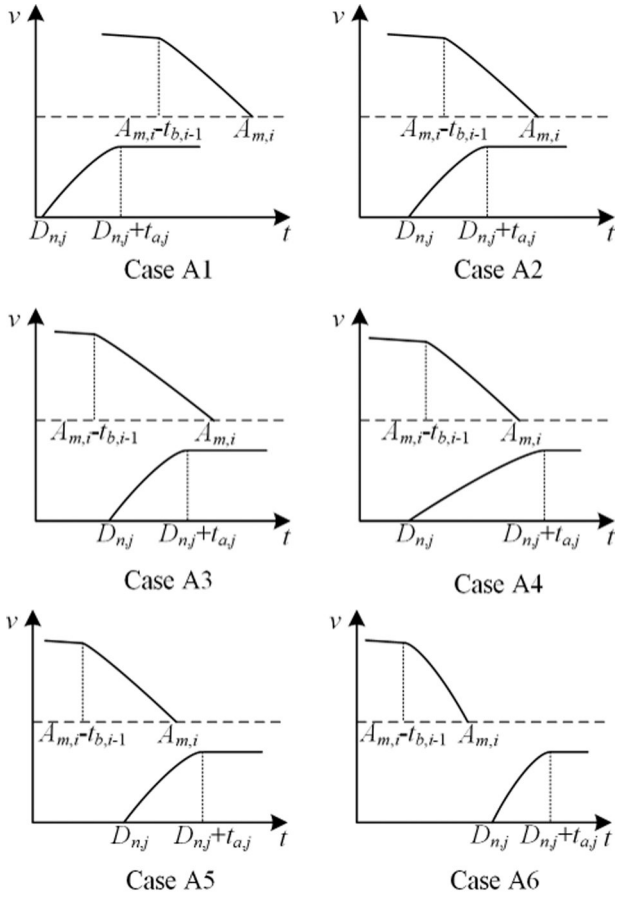

Fig. 7 *Sketch of the overlap time of the situation that train m is braking and train n is accelerating*

maximising overlap time is built under the constraints of timetable. In addition, the optimisation model is rebuilt to a MILP model with the help of logical and auxiliary variables.

4.1 Utilisation of RBE

The available RBE can be calculated as

$$J_{RBE\_a} = \sum_{i=1}^{K} \int_{S_i}^{S_{i+1}} (\eta \cdot B_E(v)) \mathrm{d}x \tag{8}$$

and, the utilised RBE can be calculated as

$$J_{RBE\_u} = \int_0^{t_{ov}} \{ \min [\eta \cdot B_E(t)v(t), F'(t)v'(t)/\eta] \} \mathrm{d}t \tag{9}$$

where $F'(t)$, $v'(t)$ is the traction force and speed of another train (kN), respectively, then the utilisation rate of RBE can be described as

$$\mu = J_{RBE\_u}/J_{RBE\_a} \tag{10}$$

According to (9), maximising the overlap time is an effective method to improve the utilisation of RBE.

4.2 Overlap time

When trains are accelerating, tractive energy can be provided by substation or the RBE from other braking trains in the same substation. Therefore, overlapping accelerating and braking phases of different trains in the same substation is an efficient way to make better use of RBE, which can reduce the energy demand from the substation.

Two successive trains (train m and train n) are used to account for the calculation of the overlap time between two successive trains, as shown in Fig. 6. When train n is accelerating and train m is braking, the RBE from train m can be utilised by train n. On the other hand, when train n is braking and train m is accelerating, the RBE from train n can be utilised by train m. The speed profile will move parallelly on the timeline by adjusting departure and arrival times, then the calculation of the overlap time will be different. The time lengths of accelerating and braking phases are determined in step 1, thus the overlap time is only influenced by departure and arrival times. According to the relationship between departure times and arrival times, the calculation of overlap time can be divided into two situations, and each situation consists of six different cases.

Situation A: train n is accelerating and train m is braking, as shown in Fig. 7. There are six different cases as follows:

Case A1: condition as

$$D_{n,j} + t_{a,j} \le A_{m,i} - t_{b,i-1} \tag{11}$$

then, the overlap time can be calculated as

$$t_{\mathrm{ov}} = 0 \tag{12}$$

Case A2: condition as

$$\begin{cases} A_{m,i} - t_{b,i-1} < D_{n,j} + t_{a,j} \le A_{m,i} \\ D_{n,j} \le A_{m,i} - t_{b,i-1} \end{cases} \tag{13}$$

then, the overlap time can be calculated as

$$t_{\mathrm{ov}} = (D_{n,j} + t_{a,j}) - (A_{m,i} - t_{b,i-1}) \tag{14}$$

Case A3: condition as

$$\begin{cases} A_{m,i} - t_{b,i-1} < D_{n,j} + t_{a,j} \le A_{m,i} \\ A_{m,i} - t_{b,i-1} < D_{n,j} \le A_{m,i} \end{cases} \tag{15}$$

then, the overlap time can be calculated as

$$t_{\mathrm{ov}} = t_{a,j} \tag{16}$$

Case A4: condition as

$$\begin{cases} A_{m,i} < D_{n,j} + t_{a,j} \\ D_{n,j} < A_{m,i} - t_{b,i-1} \end{cases} \tag{17}$$

then, the overlap time can be calculated as

$$t_{\mathrm{ov}} = t_{b,i-1} \tag{18}$$

Case A5: condition as

$$\begin{cases} A_{m,i} < D_{n,j} + t_{a,j} \\ A_{m,i} - t_{b,i-1} < D_{n,j} \le A_{m,i} \end{cases} \tag{19}$$

then, the overlap time can be calculated as

$$t_{\mathrm{ov}} = A_{m,i} - D_{n,j} \tag{20}$$

Case A6: condition as

$$A_{m,i} < D_{n,j} \tag{21}$$

then, the overlap time can be calculated as

$$t_{ov} = 0 \tag{22}$$

Situation B: train n is braking and train m is accelerating, as shown in Fig. 8. There are six different cases as follows:

Case B1: condition as

$$A_{n,j+1} \le D_{m,i} \tag{23}$$

then, the overlap time can be calculated as

$$t_{ov} = 0 \tag{24}$$

Case B2: condition as

$$\begin{cases} D_{m,i} < A_{n,j+1} \le D_{m,i} + t_{a,i} \\ A_{n,j+1} - t_{b,j} \le D_{m,i} \end{cases} \tag{25}$$

then, the overlap time can be calculated as

$$t_{ov} = A_{n,j+1} - D_{m,i} \tag{26}$$

Case B3: condition as

$$\begin{cases} D_{m,i} < A_{n,j+1} \le D_{m,i} + t_{a,i} \\ D_{m,i} < A_{n,j+1} - t_{b,j} \le D_{m,i} + t_{a,i} \end{cases} \tag{27}$$

then, the overlap time can be calculated as

$$t_{ov} = t_{b,j} \tag{28}$$

Case B4: condition as

$$\begin{cases} D_{m,i} + t_{a,i} < A_{n,j+1} \\ A_{n,j+1} - t_{b,j} \le D_{m,i} \end{cases} \tag{29}$$

then, the overlap time can be calculated as

$$t_{ov} = t_{a,i} \tag{30}$$

Case B5: condition as

$$\begin{cases} D_{m,i} + t_{a,i} < A_{n,j+1} \\ D_{m,i} < A_{n,j+1} - t_{b,j} \le D_{m,i} + t_{a,i} \end{cases} \tag{31}$$

then, the overlap time can be calculated as

$$t_{ov} = (D_{m,i} + t_{a,i}) - (A_{n,j+1} - t_{b,j}) \tag{32}$$

Case B6: condition as

$$D_{m,i} + t_{a,i} < A_{n,j+1} - t_{b,j} \tag{33}$$

then, the overlap time can be calculated as

$$t_{ov} = 0 \tag{34}$$

4.3 Model of maximising overlap time

The above cases analysis shows that the overlap time is determined by departure and arrival times. Thus, departure and arrival times are taken as decision variables to build the model of maximising overlap time. Departure and arrival times should meet the constraint of running times determined in step 1, and the constraints of headway and dwell times. When the timetable of train m is pre-given, where $m = n - 1$, the objective function of maximising overlap time between train m and train n can be described as

$$\max T_{ov} = \sum t_{ov} \tag{35}$$

subject to following timetable constraints:

(1) the constraint of departure time at the starting station

$$D_{n,1,\min} \le D_{n,1} \le D_{n,1,\max} \tag{36}$$

(2) the constraint of dwell times at middle stations

$$T_{d,j,\min} \le D_{n,j} - A_{n,j} \le T_{d,j,\max},\ j = 2, \ldots, K-1 \tag{37}$$

(3) the constraint of running times of inter-stations

$$A_{n,j} - D_{n,j-1} = T_{r,j},\ j = 2, \ldots, K \tag{38}$$

(4) the constraint of arrival time at the terminal station

$$A_{n,K,\min} \le A_{n,K} \le A_{n,K,\max} \tag{39}$$

(5) the constraint of minimum safe headway

$$\begin{cases} D_{n,j} - D_{n-1,j} \ge T_{\text{safe}} \\ A_{n,j} - A_{n-1,j} \ge T_{\text{safe}} \end{cases},\ j = 1, \ldots, N \tag{40}$$

where $D_{1,n,\min}$ and $D_{1,n,\max}$ are the minimum and maximum departure time of train n at the starting station, $T_{d,j,\min}$ and $T_{d,j,\max}$ are the minimum and maximum dwell time at the station j, $A_{K+1,n,\min}$ and $A_{K+1,n,\max}$ are the minimum and maximum arrival time of train n at the terminal station. In addition, only the overlap time between the accelerating and braking phases of trains in the same substation is considered.

4.4 Rebuild to MILP model

According to the linear characteristic of constraints (36)–(40), we plan to rebuild the model of maximising overlap time into a MILP model. However, due to the 12 cases in the calculation of overlap time, the objective function (35) is non-linear. In order to fit the framework of MILP model, logical and auxiliary variables are introduced to linearise the objective function (35). The linearisation

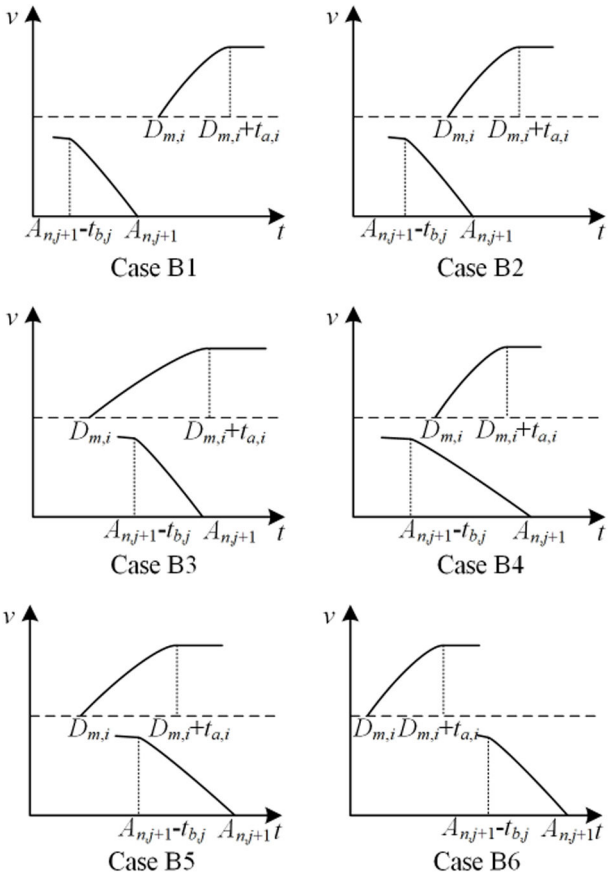

Fig. 8 *Sketch of the overlap time of the situation that train n is braking and train m is accelerating*

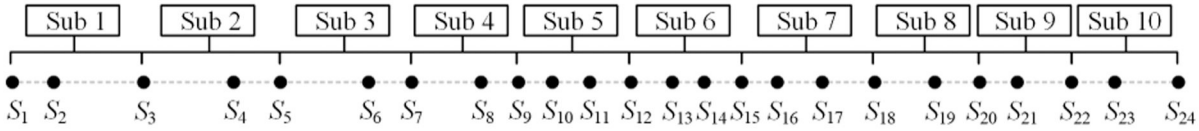

Fig. 9 *Layout of stations and substations of the metro line*

of the overlap time of Situation A is used to explain the transformation process.

Logical variables $\delta_1(j)$, $\delta_2(j)$, $\delta_3(j)$ and $\delta_4(j)$ are introduced to distinguish the relationship between the departure time of train n and the arrival time of train m, defined as

$$\begin{cases} [A_{m,i} - t_{b,i-1} \le D_{n,j}] \Leftrightarrow [\delta_1(j) = 1] \\ [D_{n,j} < A_{m,i} - t_{b,i-1}] \Leftrightarrow [\delta_1(j) = 0] \end{cases} \tag{41}$$

$$\begin{cases} [D_{n,j} + t_{a,j} \le A_{m,i}] \Leftrightarrow [\delta_2(j) = 1] \\ [A_{m,i} < D_{n,j} + t_{a,j}] \Leftrightarrow [\delta_2(j) = 0] \end{cases} \tag{42}$$

$$\begin{cases} [A_{m,i} - t_{b,i-1} \le D_{n,j} + t_{a,j}] \Leftrightarrow [\delta_3(j) = 1] \\ [D_{n,j} + t_{a,j} < A_{m,i} - t_{b,i-1}] \Leftrightarrow [\delta_3(j) = 0] \end{cases} \tag{43}$$

$$\begin{cases} [D_{n,j} \le A_{m,i}] \Leftrightarrow [\delta_4(j) = 1] \\ [D_{n,j} < A_{m,i}] \Leftrightarrow [\delta_4(j) = 0] \end{cases} \tag{44}$$

The above logical conditions can be rewritten as the form of inequalities [30]. For example, the logical condition (41) can be rewritten as

$$\begin{cases} (A_{m,i} - t_{b,i-1} - T_{\max})\delta_1(j) + D_{n,j} \le A_{m,i} - t_{b,i-1} \\ (A_{m,i} - t_{b,i-1} + \varepsilon - T_{\min})\delta_1(j) - D_{n,j} \le -T_{\min} \end{cases} \tag{45}$$

where $T_{\min}$ is the minimum value of $D_{n,j}$, $T_{\max}$ is the maximum value of $D_{n,j}$, ε is a small positive value to transform a strict inequality into an inequality. Logical conditions (42)–(44) can be rewritten in the same way as inequality (45). Furthermore, with the help of logical variables, the overlap time t_{ov} of Situation A can be described as

$$\begin{aligned} t_{\text{ov}} = \delta_3\delta_4[\delta_2(D_{n,j} + t_{a,j}) + (1 - \delta_2)A_{m,i} \\ -\delta_1 D_{n,j} - (1 - \delta_1)(A_{m,i} - t_{b,i-1})] \end{aligned} \tag{46}$$

However, there are products of two logical variables in (46), like $\delta_3\delta_4$, and products of logical variables and decision variable, like $\delta_3\delta_4\delta_2 D_{n,j}$, which are not suitable for the framework of MILP model. By defining auxiliary variables to replace these products, the non-linear equation (46) can be transformed into a linear equation. For the product $\delta_3\delta_4$, auxiliary variable $\delta_5 = \delta_3\delta_4$ is introduced, defined as

$$\begin{cases} -\delta_3 + \delta_5 \le 0 \\ -\delta_4 + \delta_5 \le 0 \\ \delta_3 + \delta_4 - \delta_5 \le 1 \end{cases} \tag{47}$$

Similarly, variables $\delta_6 = \delta_1\delta_5$ and $\delta_7 = \delta_2\delta_5$ can be defined in the same way as (47). Meanwhile, for the product $\alpha_1 = \delta_6 D_{n,j}$, auxiliary variable α_1 is introduced, defined as

$$\begin{cases} -T_{\max}\delta_6 + \alpha_1 \le 0 \\ T_{\min}\delta_6 - \alpha_1 \le 0 \\ -T_{\min}\delta_6 + \alpha_1 - D_{n,i} \le -T_{\min} \\ T_{\max}\delta_6 - \alpha_1 + D_{n,i} \le T_{\max} \end{cases} \tag{48}$$

Similarly, auxiliary variable $\alpha_2 = \delta_7 D_{n,j}$ can be defined in the same way as (48). Then, the overlap time t_{ov} can be described as a linear function

$$t_{ov} = t_{b,i-1}\delta_5 + (A_{m,i} - t_{b,i-1})\delta_6 + (t_{a,j} - A_{m,i})\delta_7 - \alpha_1 + \alpha_2 \tag{49}$$

Similarly, logical variables η_1, η_2, η_3, η_4, η_5, η_6, η_7 and auxiliary variables β_1 β_2 are introduced to linearise the overlap time t_{ov} of Situation B. Then, the overlap time t_{ov} of Situation B can also be described as a linear function

$$t_{\text{ov}} = t_{a,i}\eta_5 + (D_{m,i} + t_{b,j})\eta_6 + (-D_{m,i} - t_{a,i})\eta_7 - \beta_1 + \beta_2 \tag{50}$$

With the help of logical and auxiliary variables, the model of maximising overlap time can be rebuilt to a MILP model. Some decision variables are defined as

$$D = \begin{bmatrix} D_1 \\ D_2 \\ \vdots \\ D_K \end{bmatrix}, \quad A = \begin{bmatrix} A_2 \\ A_3 \\ \vdots \\ A_{K+1} \end{bmatrix}, \quad \delta_1 = \begin{bmatrix} \delta_1(1) \\ \delta_1(2) \\ \vdots \\ \delta_1(K) \end{bmatrix}, \quad \alpha_1 = \begin{bmatrix} \alpha_1(1) \\ \alpha_1(2) \\ \vdots \\ \alpha_1(K) \end{bmatrix}$$

and, other logical and auxiliary variables can be defined in the same way as the definitions of δ_1 and α_1, respectively. Furthermore, the decision matrix of the MILP model can be defined as

$$X = [D^T A^T \delta_1^T \cdots \delta_7^T \alpha_1^T \alpha_2^T \eta_1^T \cdots \eta_7^T \beta_1^T \beta_2^T]^{\mathrm{T}}$$

then, the MILP model of maximising overlap time can be obtained as

$$\min\ CX \tag{51}$$

subject to

$$M_1 X \le m_1 \tag{52}$$

$$M_2 X = m_2 \tag{53}$$

where the objective coefficient C can be defined according to (49) and (50), inequality constraints coefficient M_1 and m_1 can be defined according to (36), (37), (39), (40), (45), (47) and (48), and equality constraints coefficient M_2 and m_2 can be defined according to (38).

The MILP model can be solved by branch-and-bound algorithms implemented in several existing commercial and free solvers. In this paper, CPLEX solver is used to solving the MILP model.

5 Simulations

5.1 Simulation parameters

A Guangzhou Metro Line is involved in the simulations. The metro line consists of 24 stations and 10 substations, the layout of stations and substations is shown in Fig. 9. Speed limit and change of gradient are shown in Fig. 10. Temporary and permanent speed limits are both considered. PRTs of each inter-station are shown in Table 2, and pre-given dwell times are shown in Table 3. The train running in the metro line is A-type EMU with the mass of 339.6 t, the factor considering the rotating mass is 0.08, the efficiency of the train motor is 0.85. The maximum traction force is described as

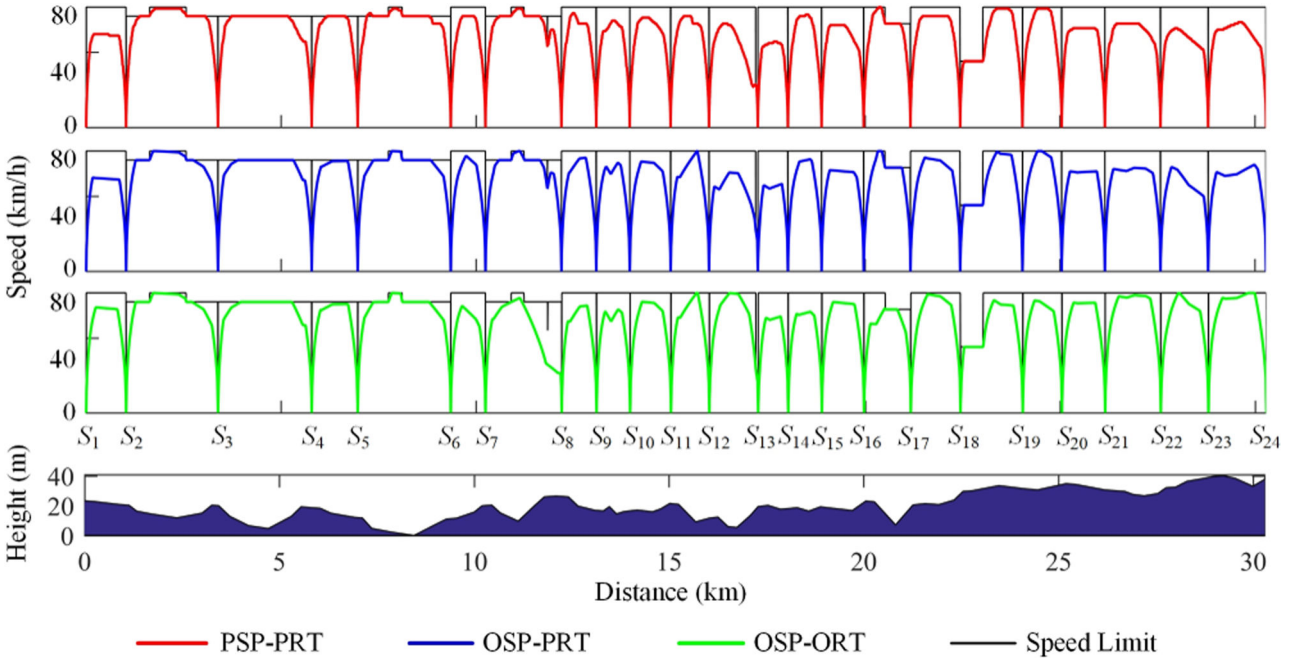

Fig. 10 *Speed profiles and change of gradient*

Table 2 Running times of PRT and ORT (s)

Starting station	S_1	S_2	S_3	S_4	S_5	S_6	S_7	S_8	S_9	S_{10}	S_{11}	S_{12}
PRT	77	135	140	80	138	65	119	66	65	74	71	97
ORT	73	135	141	80	139	68	153	67	66	73	71	85

Starting station	S_{13}	S_{14}	S_{15}	S_{16}	S_{17}	S_{18}	S_{19}	S_{20}	S_{21}	S_{22}	S_{23}
PRT	67	64	77	82	87	117	69	80	95	92	100
ORT	65	66	74	86	85	119	71	77	88	83	92

Table 3 Dwell times of four timetable plans (s)

Timetable type	Train	S_2	S_3	S_4	S_5	S_6	S_7	S_8	S_9	S_{10}	S_{11}	S_{12}
PSP/OSP-PT	the second	30	31	39	34	36	33	45	53	42	37	39
	the third	30	31	39	34	36	33	45	53	42	37	39
PSP-OT	the second	36	37	31	27	29	26	36	42	34	41	47
	the third	36	26	31	27	29	26	54	47	34	30	31
OSP-OT	the second	24	26	31	27	29	26	36	42	44	44	47
	the third	24	35	31	27	35	40	36	42	34	30	31

Timetable type	Train	S_{13}	S_{14}	S_{15}	S_{16}	S_{17}	S_{18}	S_{19}	S_{20}	S_{21}	S_{22}	S_{23}
PSP/OSP-PT	the second	56	38	36	64	41	39	32	41	42	41	44
	the third	56	38	36	64	41	39	32	41	42	41	44
PSP-OT	the second	67	33	43	51	39	47	38	41	50	49	35
	the third	45	46	38	51	49	47	38	49	50	49	35
OSP-OT	the second	67	46	43	51	33	31	29	49	50	46	35
	the third	58	46	43	51	33	31	33	49	34	48	40

(54). The maximum regenerative braking force is described as (55). The maximum air braking is 400 kN, for $0 < v < 5$ km/h. The basic resistance is described as (56), and the parameter k is 6.38. Simulations are tested under the MATLAB environment on a computer with Intel Core i5 2.30 GHz CPU and 8 GB RAM, and the MILP model is solved by using CPLEX Solver 12.6.

$$F_{\max}(v) = \begin{cases} 400 & 0 < v \le 40 \\ 1600/v & 40 < v \le 55 \\ 88, & 000/v^2 55 < v \le 80 \end{cases} \tag{54}$$

$$B_{E,\max}(v) = \begin{cases} 0 & 0 < v \le 3 \\ 194.5(v-3) & 3 < v \le 5 \\ 389 & 5 < v \le 48.5 \\ 913,953/v^2 & 48.5 < v \le 80 \end{cases} \tag{55}$$

$$W_0(v) = 9.067 + 0.0173v^2 \quad (56)$$

5.2 Simulation of speed profile optimisation

In this simulation, the speed profile of an inter-station with steep downhill and low-speed limit is optimised by the proposed coasting point searching algorithm. Meanwhile, the influence of the value of parameter Δx is analysed. Two optimal speed profiles are discussed in this simulation, as follows:

- OSP ($\Delta x = 1$ m): optimal speed profile with $\Delta x = 1$ m;
- OSP ($\Delta x = 10$ m): optimal speed profile with $\Delta x = 10$ m.

The speed limit and change of gradient of the inter-station are shown in Fig. 11. The MaxPow speed profile, OSP ($\Delta x = 1$ m) and OSP ($\Delta x = 10$ m) are shown in Fig. 11. The performance of two optimal speed profiles is shown in Table 4. As shown in Fig. 11, the speed profile of the inter-station is divided into three subintervals, where THE CO phases are added to. The formulation of the first subinterval is due to the steep downhill. The formulation of the latter two subintervals is due to the low-speed limit. According to the performance of two optimal speed profiles, the starting positions of CO phases are different due to the different value of Δx. The running times of two optimal speed profiles are all meet the constraint of the PRT, and the running time of OSP ($\Delta x = 1$ m) is closer to the PRT. Furthermore, the tractive energy consumption of OSP ($\Delta x = 1$ m) is lower compared with OSP ($\Delta x = 10$ m). The computing time of OPS ($\Delta x = 10$ m) is lower than the computing time of OPS ($\Delta x = 1$ m). However, the calculation only needs to be offline in this paper, thus Δx is set to 1 m, which can make the speed profile optimisation more energy-saving.

5.3 Simulation of minimising tractive energy consumption

In this simulation, the speed profiles and running time distribution of the metro line are optimised by the method proposed in step 1. Firstly, the speed profiles of each inter-station are optimised with the PRT distribution scheme. Secondly, the speed profiles and running time distribution scheme are optimised jointly. Meanwhile, the practical speed profiles (PSPs) with PRT distribution scheme are introduced to compare with the optimisation results. Three different operation plans are discussed in this section, as follows:

- PSP-PRT: PSPs with PRT distribution scheme.
- OSP-PRT: PSPs with PRT distribution scheme.
- OSP-ORT: PSPs with optimal running time (ORT) distribution scheme.

Speed profiles of three operation plans are shown in Fig. 10. Total running times and tractive energy consumption of three operation plans are shown in Table 5. PRT distribution scheme and ORT distribution scheme are shown in Table 2. As shown in Fig. 10, optimal speed profiles meet the constraint of speed limit. For the PSP, the CO phases are also added into the driving strategy, like the speed profile of the inter-station $[S_{15}, S_{16}]$. With the application of the proposed coasting point searching algorithm, the total tractive energy consumption of OSP-PRT is reduced by 6.16% compared with PSP-PRT. In addition, when the optimisation of running time distribution is considered, the total tractive energy consumption of OSP-ORT is reduced by 8.46% compared with PSP-PRT without changing the total running time. The energy-saving effect is improved by 2.30% comparing OSP-PRT with OSP-ORT, which implies that the optimisation of running time distribution scheme can further reduce tractive energy consumption.

5.4 Simulation of maximising overlap time

In this simulation, the timetable of three trains is optimised by the method proposed in step 2. The pre-given headway of trains is 200 s. The fluctuating value of departure time at the starting station is set to 40 s, i.e. $D_{1,n,\max} = D_{1,n} + 20$, $D_{1,n,\min} = D_{1,n} - 20$. The fluctuating value of dwell time is set to 20 s, i.e. $T_{\mathrm{d},j,\max} = T_{\mathrm{d},j} + 10$, $T_{\mathrm{d},j,\min} = T_{d,j} - 10$ for $j = 2,\ldots,K\text{-}1$. The fluctuating value of arrival time at the ending station is set to 40 s, i.e. $A_{K,n,\max} = A_{K,n} + 20$, $A_{K,n,\min} = A_{K+1,n} - 20$. The minimum safe headway is 90 s. Running times and time lengths of accelerating and braking phases are determined based on the practical and optimal speed profiles in step 1. The first train departs from the starting station at the moment 0 s, and the departure and arrival times of the first train are determined based on the pre-given timetable. The departure and arrival times of the second train and the third train are optimised with the help of the proposed method. Four different timetable plans are discussed in this simulation, as follows:

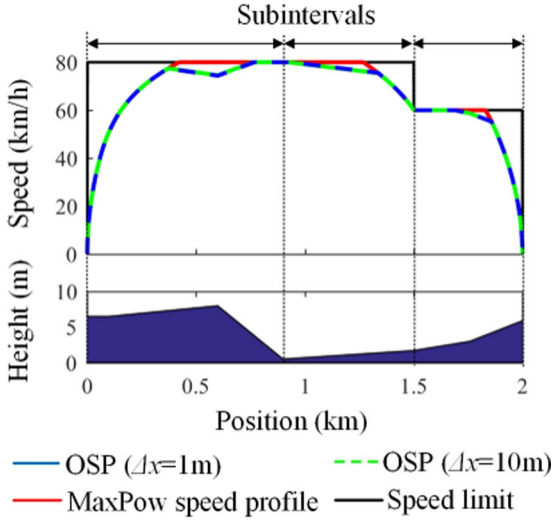

Fig. 11 *Three kinds of speed profiles of the inter-station with steep downhill*

Table 4 Performance of two speed profiles of the inter-station

Speed profile type	OSP ($\Delta x = 1$)	OSP ($\Delta x = 10$ m)
starting position of CO phases, m	373, 924, 1689	371, 939, 1690
running time, s	122.99	122.98
tractive energy consumption, kWh	32.54	32.57
computing time, s	3.74	0.40

where the PRT is 123 s.

Table 5 Total running times and total tractive energy consumption of three operation plans

Operation plan	T_T, s	J_t, kWh
PSP-PRT	2057	655.17
OSP-PRT	2057	614.84
OSP-ORT	2057	599.73

- PSP-PT: PSP with pre-given timetable.
- PSP-OT: PSP with optimal timetable, where dwell times and headway are optimised.
- OSP-PT: optimal speed profile with pre-given timetable, where speed profile and running times are optimised.
- OSP-OT: optimal speed profile with optimal timetable, where speed profile, running times, dwell times and headway are optimised.

Dwell times of four timetable plans are shown in Table 3. Headway and overlap times of four timetable plans are shown in Table 6. Energy consumption of three timetable plans is shown in Table 7. The optimisation results show that the total overlap time of PSP can be improved by 69.78% comparing PSP-PT with PSP-OT, and the total overlap time of OSP can be improved by 121.34% comparing OSP-PT with OSP-OT. The improvement of the overlap time is realised by adjusting headway and dwell times without

Table 6 Overlap times and headway of four timetable plans (s)

Timetable type	Overlap time			Headway	
	The first and second train	The second and third train	Total	The first and second train	The second and third train
PSP-PT	122.6	122.6	245.2	200	200
PSP-OT	233.8	182.5	416.3	218	220
OSP-PT	88.1	88.1	176.2	200	200
OSP-OT	197.0	193.0	390.0	220	210

Table 7 Energy consumption performance of four timetable plans, kWh

Timetable type	Available RBE	Utilised RBE	Utilisation rate of RBE, %	Total tractive energy consumption	Total operational energy consumption
PSP-PT	1080.81	312.35	28.9	1965.51	1653.16
PSP-OT	1080.81	436.65	40.4	1965.51	1528.86
OSP-PT	1019.64	261.03	25.6	1844.52	1583.49
OSP-OT	908.01	337.78	37.2	1799.19	1461.41

changing running time or speed profile. The increase in the overlap time improves the utilisation of RBE. The optimisation results show that the utilisation rate of RBE of PSP can be improved by 11.5% comparing PSP-PT with PSP-OT, and the utilisation rate of OSP can be improved by 11.6% comparing OSP-PT with OSP-OT, which implies that the method proposed is effective to make better use of the RBE. Meanwhile, the total train operational energy consumption is reduced effectively as shown in Table 7.

5.5 Feasibility of optimisation results

The optimisation results demonstrate that the proposed methods can reduce the operational energy consumption of metro transit system effectively. In addition, the optimisation results can be applied in practical operation.

Firstly, the optimal speed profiles meet the constraint of speed limit, which ensures the safety of operation, as shown in Fig. 11. Meanwhile, when the running time of the inter-station is given, the optimal speed profile can meet the constraints of running time, which ensures the punctuality of operation, as shown in Table 4. Therefore, the optimal speed profile calculated by the proposed coasting point searching algorithm can be applied in practice.

Secondly, for each inter-station, the running times of the running time distribution scheme are all bigger than the minimum running times. Meanwhile, the adjustment of departure and arrival times is under constraints (36)–(40), which keeps headway and dwell times within reasonable bounds. Therefore, the optimal timetable is appropriate and acceptable in practice.

6 Conclusion

In this paper, a two-step optimisation method is proposed to reduce tractive energy consumption and improve the utilisation of RBE. In step 1, energy-efficient speed profiles and running time distribution scheme are jointly optimised by a novel coasting point searching algorithm in order to reduce tractive energy consumption. In step 2, the overlap time between the accelerating and braking phases is introduced to measure the utilisation of RBE. A timetable optimisation model is built to maximise the overlap time by adjusting headway and dwell time. Meanwhile, a timetable optimisation model is rebuilt into a MILP model, which can be solved efficiently by CPLEX Solver. Based on practical data from a Guangzhou Metro Line, some numerical simulations are performed to demonstrate the effectiveness of the presented method. The results show that the total tractive energy consumption can be reduced by 8.46%, and the utilisation of RBE can be improved by 11.5 and 11.6% for PSP and optimal speed profile, respectively. Therefore, the proposed two-step method can reduce the operational energy consumption of metro transit system effectively by optimising speed profile and timetable.

Even though the proposed two-step optimisation method is proven to be efficient in the numerical simulations, optimisation results from the proposed method are suboptimal. In future work, speed profile and timetable should be optimised simultaneously to get the global optimal solution, and the coordination of trains in the opposite direction should be considered. On the other hand, the utilisation of RBE is roughly measured by the overlap time, which is imprecise. The model of the power supply system should be built to measure the utilisation of RBE more precisely.

7 Acknowledgments

This work was supported in part by the Fundamental Research Funds for the Central Universities of China under grant no. 2682017CX048 and in part by the National Key Research and Development Program of China under 2017YFB1201302-09.

8 References

[1] Yang, X., Li, X., Ning, B., *et al.*: 'A survey on energy-efficient train operation for urban rail transit', *IEEE Trans. Intell. Transp. Syst.*, 2016, **17**, (1), pp. 2–13

[2] Scheepmaker, G.M., Goverde, R.M.P., Kroon, L.G.: 'Review of energy-efficient train control and timetabling', *Eur. J. Oper. Res.*, 2017, **257**, (2), pp. 355–376

[3] Ishikawa, K.: 'Application of optimization theory for bounded state variable problems to the operation of trains', *Bull. JSME*, 1968, **11**, (47), pp. 857–865

[4] Howlett, P.G.: 'An optimal strategy for the control of a train', *Aust. Math. Soc.*, 1990, **31**, (4), pp. 454–471

[5] Pudney, P.J., Howlett, P.G.: 'Optimal driving strategies for a train journey with speed limits', *J. Aust. Math. Soc. Ser. B-Appl. Math.*, 1994, **36**, pp. 38–49

[6] Albrecht, A.R., Howlett, P.G., Pudney, P.J., *et al.*: 'Energy-efficient train control: from local convexity to global optimization and uniqueness', *Automatica*, 2013, **49**, (10), pp. 3072–3078

[7] Franke, R., Terwiesch, P., Meyer, M.: 'An algorithm for the optimal control of the driving of trains'. Proc. IEEE Conf. Decision Control, Sydney, Australia, 2000, vol. 3, pp. 2123–2128

[8] Wang, Y., De Schutter, B., Ning, B., *et al.*: 'Optimal trajectory planning for trains using mixed integer linear programming'. 14th Int. IEEE Conf. Intelligent Transportation Systems, Washington, USA, 2011, vol. 19, pp. 1598–1604

[9] Zhao, N., Chen, L., Tian, Z., *et al.*: 'Field test of train trajectory optimisation on a metro line', *IET Intell. Transp. Syst.*, 2017, **11**, (5), pp. 273–281

[10] Lechelle, S.A., Mouneimne, Z.S.: 'Optidrive: A practical approach for the calculation of energy-optimised operating speed profile'. Proc. IET Conf. Railway Traction Systems, Birmingham, UK, 2010, vol. 44, pp. 1–8

[11] Lu, S., Hillmansen, S., Ho, T., *et al.*: 'Single-train trajectory optimization', *IEEE Trans. Intell. Transp. Syst.*, 2013, **14**, (2), pp. 743–750

[12] Wong, K., Ho, T.: 'Coast control for mass rapid transit railways with searching methods', *IEE Proc. Electr. Power Appl.*, 2004, **151**, (3), pp. 365–376

[13] Chang, C.S., Sim, S.S.: 'Optimising train movements through coast control using genetic algorithms', *IEE Proc. Electr. Power Appl.*, 1997, **144**, (1), pp. 65–73

[14] Su, S., Li, X., Tang, T., *et al.*: 'A subway train timetable optimization approach based on energy-efficient operation strategy', *IEEE Trans. Intell. Transp. Syst.*, 2013, **14**, (2), pp. 883–893

[15] Sicre, C., Cucala, P., Fernández, A., *et al.*: 'A method to optimise train energy consumption combining manual energy efficient driving and scheduling', *WIT Trans. Built Environ.*, 2010, **114**, pp. 549–560

[16] Vandanjon, P., Lejeune, A., Chevrier, R., *et al.*: 'Towards eco-aware timetabling: evolutionary approach and cascading initialisation strategy for the bi-objective optimisation of train running times', *IET Intell. Transp. Syst.*, 2016, **10**, (7), pp. 483–494

[17] González-Gil, A., Palacin, R., Batty, P., *et al.*: 'A systems approach to reduce urban rail energy consumption', *Energy Convers. Manag.*, 2014, **80**, pp. 509–524

[18] Liu, J., Guo, H., Yu, Y.: 'Research on the cooperative train control strategy to reduce energy consumption', *IEEE Trans. Intell. Transp. Syst.*, 2016, **1**, (5), pp. 1–9
[19] Albrecht, T.: 'Reducing power peaks and energy consumption in rail transit systems by simultaneous train running time control', *Computers in Railways IX*, (WIT Press, Southampton, UK., 2014), pp. 885–894
[20] Ramos, A., Pena, M., Fernández-Cardador, A.*, et al.*: 'Mathematical programming approach to underground timetabling problem for maximizing time synchronization'. Proc. Int. Conf. Industrial Engineering and Industrial Management, Madrid, Spain, 2007, pp. 88–95
[21] Yang, X., Chen, A., Li, X.*, et al.*: 'An energy-efficient scheduling approach to improve the utilization of regenerative energy for metro systems', *Transp. Res. Part C Emerg. Technol.*, 2015, **57**, pp. 13–29
[22] Ning, J., Zhou, Y., Long, F.*, et al.*: 'A synergistic energy-efficient planning approach for urban rail transit operations', *Energy*, 2018, **151**, pp. 854–863
[23] Li, X., Lo, H.K.: 'An energy-efficient scheduling and speed control approach for metro rail operations', *Transp. Res. B, Methodol.*, 2014, **64**, pp. 73–89
[24] Zhao, N., Roberts, C., Hillmansen, S.: 'An integrated metro operation optimization to minimize energy consumption', *Transp. Res. Part C Emerg. Technol.*, 2017, **75**, pp. 168–182
[25] Yang, S., Wu, J., Sun, H.*, et al.*: 'Bi-objective nonlinear programming with minimum energy consumption and passenger waiting time for metro systems, based on the real-world smart-card data', *Transp. Res. B, Methodol.*, 2018, **6**, (4), pp. 1–18
[26] Gao, Y., Yang, L., Gao, Z.: 'Energy consumption and travel time analysis for metro lines with express/local mode', *Transp. Res. D, Transp. Environ.*, 2016, **60**, pp. 7–27
[27] Zhou, Y., Bai, Y., Li, J.*, et al.*: 'Integrated optimization on train control and timetable to minimize net energy consumption of metro lines', *J. Adv. Transp.*, 2018, **2018**, pp. 1–19
[28] Su, S., Tang, T., Roberts, C.: 'A cooperative train control model for energy saving', *IEEE Trans. Intell. Transp. Syst.*, 2015, **16**, (2), pp. 622–631
[29] Wang, P., Goverde, R. M. P.: 'Multi-train trajectory optimization for energy-efficient timetabling', *Eur. J. Oper. Res.*, 2019, **271**, (2), pp. 621–635
[30] Bemporad, A., Morari, M.: 'Control of systems integrating logic, dynamics, and constraints', *Automatica*, 1999, **35**, (3), pp. 407–427